The association for medical ultrasound
aium
AMERICAN INSTITUTE OF ULTRASOUND IN MEDICINE

Still Time to Attend ONLINE!

46th Annual

Advanced OB&GYN Ultrasound Seminar

EARN UP TO 20.5

Focused on Your Toughest Diagnostic Challenges

February 15–18, 2023 | **Disney's Yacht and Beach Club Resorts • Lake Buena Vista, Florida**

Preseminar: February 15: Principles of Sonography and Doppler Ultrasound

World-Class Faculty

Program Leaders

Alfred Z. Abuhamad
MD, FAIUM
Co-Director

Beryl Benacerraf
MD, FAIUM
Co-Director in Memoriam

Founders

Lennard D. Greenbaum
MD, FAIUM
Director Emeritus

Frederick W. Kremkau
PhD, FAIUM
Director Emeritus

Brett D. Einerson
MD, MPH

Yvette S. Groszmann
MD, MPH, FAIUM

Lawrence D. Platt
MD, FAIUM

Elena Sinkovskaya
MD, PhD, FAIUM

Joanne Stone
MD, MS

Cutting-edge Sessions & Topics

- Abnormal Uterine Bleeding
- Adnexal Masses
- Complicated Multiple Gestations
- Diagnosing Genetic Syndromes
- Fetal Chest Malformations
- Fetal Growth Restriction
- Imaging of the Fetal Brain
- Imaging of the Fetal Heart
- Pelvic Pain

IN PROUD PARTNERSHIP WITH

ORLANDO HEALTH

Wake Forest® School of Medicine

View full agenda and register at
aium.org/OBGYNseminar

Comparison of Ultrasonography to MRI in the Diagnosis of Lower Extremity Bone Stress Injuries

A Prospective Cohort Study

Isaac Syrop, MD, Yaeko Fukushima, MD PhD, Kevin Mullins, MD, Sara Raiser, MD, Richard Lawley, MD, Lauren Bosshardt, MD, Andrea Finlay, PhD, Jeremiah Ray, MD, Michael Fredericson, MD

Received February 22, 2021, from the Department of Rehabilitation and Regenerative Medicine, Columbia University Vagelos College of Physicians and Surgeons, New York, NY, USA (I.S.); Department of Physical Medicine and Rehabilitation, Kansai Medical University, Osaka, Japan (Y.F.); Department of Physical Medicine and Rehabilitation, UC Davis, Davis, CA, USA (K.M.); Department of Orthopaedics, Emory University, Atlanta, GA, USA (S.R.); Sports Medicine, Orthopedic Centers of Colorado, Denver, CO, USA (R.L.); Emergency Medicine, Prisma Health Upstate, Greenville, SC, USA (L.B.); Department of Orthopaedic Surgery, Division of Physical Medicine and Rehabilitation, Stanford University School of Medicine, Stanford, CA, USA (A.F., M.F.); and Hoag Medical Group, Foothill Ranch, CA, USA (J.R.). Manuscript accepted for publication February 5, 2022.

Isaac Syrop and Yaeko Fukushima share co-first authorship.

Address correspondence to Michael Fredericson, MD, FACSM, PM&R Sports Medicine, Division of PM&R, Department of Orthopaedic Surgery, Stanford University School of Medicine, 450 Broadway Street, Pavilion A, 2nd Floor MC 6120, Redwood City, CA 94063, USA.

E-mail: mfred2@standford.edu

Isaac Syrop, MD, PM&R Sports Medicine, Department of Rehabilitation and Regenerative Medicine, Columbia University Vagelos College of Physicians and Surgeons, 1985 Crompond Road, Building E, Cortlandt Manor, NY 10567, USA.

E-mail: ips2109@cumc.columbia.edu

Abbreviations

BSI, bone stress injury; CT, computed tomography; MRI, magnetic resonance imaging; USI, ultrasound imaging

doi:10.1002/jum.15977

Objective—To determine the sensitivity and specificity of ultrasound imaging (USI) compared to the reference-standard of MRI in the diagnosis of bone stress injury (BSI).

Methods—A prospective blinded cohort study was conducted. Thirty seven patients who presented to an academic sports medicine clinic from 2016 to 2020 with suspected lower-extremity BSI on clinical exam underwent both magnetic resonance imaging (MRI) and USI. Participant characteristics were collected including age, gender and sport. Exclusion criteria included contraindication for dedicated MRI, traumatic fracture, or severe tendon or ligamentous injury. The primary outcome measure was BSI diagnosis by USI. An 8-point assessment system was utilized on USI for diagnosis of BSI, and the Fredericson and Nattiv[22] criteria were applied to classify MRI findings.

Results—Thirty seven participants who met study criteria were consented to participate. All participants completed baseline measures. Using MRI, there were 30 (81%) athletes with a positive and seven participants with a negative BSI diagnosis. The most common BSIs in the study were in the metatarsal (54%) and tibia (32%). Compared to MRI, USI demonstrated 0.80 sensitivity (95% confidence interval [CI], 0.61–0.92) and 0.71 specificity (95% CI, 0.29–0.96) in detecting BSI, with a positive predictive value of 0.92 (95% CI, 0.75–0.99) and negative predictive value of 0.45 (95% CI, 0.17–0.77).

Conclusions—USI is a potentially useful point-of-care tool for practicing sports medicine providers to combine with their clinical evaluation in the diagnosis of BSIs. Further research is ongoing to determine the role of USI in follow-up care and return-to-play protocols.

Key Words—bone stress injuries; ultrasound; stress fractures; diagnosis; ultrasonography; MRI

Bone stress injuries (BSIs) are relatively common in college-level athletes and can result in substantial disability leading to prolonged leave from sport when diagnosed in more advanced stages. Collectively, BSIs account for 0.7 to 20% of all injuries seen in sports medicine clinics,[1] with a prevalence of up to 28.9% in higher-risk female athletic populations, such as track and field.[2–4] Approximately 90% of all BSIs occur within the lower extremity,[5–7] a testament to the repetitive mechanical loading that bones endure during various sporting activities, which can result in

structural fatigue and localized pain over a prolonged period of time.[8,9] Such BSIs however cannot be confined to one distinct pathological entity; rather, these injuries represent a continuum of disease severity. The presence of a cortical fracture line on imaging for example, or lack thereof can help to delineate between the diagnosis of a stress reaction from that of a more significant and advanced stress fracture.[10,11]

In clinical practice, early diagnosis of BSI is imperative to allow for judicious implementation of appropriate restful treatment and avoidance of substantially longer healing times required for higher-grade injuries.[12] Therefore, a readily accessible point-of-care imaging device that can be reasonably utilized as a diagnostic tool for healthcare providers in the diagnosis of BSIs is essential. Radiographic identification of BSIs is the least sensitive method for detecting low-grade BSIs, resulting in a high false negative rate (85%).[13] Meanwhile, alternative options such as computed tomography (CT) is poor at detecting early injury, while bone scintigraphy will not evaluate for cortical break, and both of these imaging options are costly and expose patients to ionizing radiation.[14,15] As a result, MRI has emerged since the 1980s as the diagnostic reference standard for many practitioners in confirming BSIs, given the high sensitivity and specificity that MRI conveys in detecting cortical fracture precursors, such as periosteal reaction and bone marrow edema.[16–19]

Fredericson and colleagues[20] described an MRI grading scale for tibial BSIs in 1995, which has since been developed by Adrent and Griffiths[21] in 1997, and Nattiv et al in 2013,[22] to encompass all BSIs, currently serving as the reference standard for diagnosis. Although the MRI classification system has been validated for determining return to sport times,[23] routine use of MRI remains both expensive and time-consuming, for many clinical scenarios. Thus, there is good reason to believe that the more affordable and accessible diagnostic option of musculoskeletal USI may help to address the shortcomings of MRI.

Howard and colleagues[24] published the first manuscript of diagnostic musculoskeletal USI for the detection of a stress fracture in 1992, describing a small periosteal elevation in the patient's second metatarsal bone. Later contributions to the literature by Caruso et al[25] in 2000 and Rawool et al[26] in 2003, discussed the addition of color Doppler and power Doppler respectively, both of which have helped to pave the way for establishing modern-day sonographic biomarkers important in assessing BSIs.

Yet, while previous investigations have explored the use of USI in the diagnosis of BSIs, such studies have done so with inconsistent measures applied, resulting in a wide array of scientific conclusions.[27–31] In a systematic review of the diagnostic accuracy of imaging modalities for suspected lower extremity BSIs, Wright and colleagues[32] reported a wide-ranging sensitivity of 43 to 99% and specificity of 13 to 79%. There is longstanding interest within the sports medicine community of the potential diagnostic accuracy for USI in the detection of BSI, yet there is not currently a common and concise set of criteria to use for BSI diagnosis.[33–37] The purpose of our study was to determine the ultrasound diagnostic markers that are most sensitive and specific for the detection of BSIs, with MRI as the reference standard, among a young and healthy athletic population.

Methods

Participants

A prospective observational cohort study was conducted in the Stanford Physical Medicine & Rehabilitation Sports Medicine Clinics (Palo Alto, CA), between 2016 and 2020. Inclusion criteria was clinical suspicion of a lower extremity BSI. Clinical suspicion was broadly defined as localized mechanical pain overlying bone, increased by local loading and relieved by rest. Exclusion criteria included contraindication for dedicated MRI or a history that indicated a traumatic fracture or severe tendon or ligamentous injury. Anatomic locations not adequately assessed using ultrasound were excluded, such as the hip and pelvis. This research was approved by the Academic Hospital's Institutional Review Board, participants provided written informed consent, the study was HIPAA-compliant, and all authors declare that they have no conflicts of interest.

Procedure

All participants underwent history and physical examination the same day of visiting the sports medicine clinic and underwent USI and MRI within 1 week of presentation. History included age, gender, sport, chief complaint and prior history of BSI. Physical Examination included the presence or absence of pain

with bony palpation, percussion, rest, walking. MRIs were read by Stanford musculoskeletal radiologists. The USI was performed using the Konica Minolta HS-1 ultrasound machine (Tokyo, Japan) with a 4–18 MHz high frequency linear transducer. Exams were performed over the identified location of pain, overlying bone, from proximal to distal and medial to lateral, in both long axis and short axis. Throughout the study duration, a total of five sonologists performed the scans, with each read by the performing sonologist and one additional physician blinded to the findings of the other examiner, before agreement was achieved. A third physician was used in cases of discrepancy. The total duration of each USI assessment was approximately 20 min. Sonologists with ACGME Sports Medicine fellowship training performed the scans, all of whom were experienced in musculoskeletal USI, with years of experience ranging from 4 to 12. None of the sonologists had access to the radiologic and/or MRI findings and were only made aware of the clinical finding of pain location.

Sonographic biomarkers recorded were based on the criteria set by Bianchi and Luong,[30] denoting thickening of the periosteum, presence of a calcified bone callus, cortical irregularities, subcutaneous edema, and color/power Doppler hypervascular changes of the periosteum, subcutaneous soft tissues, and intraosseous bone. Doppler gain was optimized for low flow with a setting just below the level that produces random noise, and frequency was 8 to 13 MHz. Additional biomarkers included complete cortical disruption, periosteal elevation and periosteal hypoechogenicity (Table 1). Periosteal hypoechogenicity was distinguished from periosteal thickening, with the former defined as a region of hypoechogenicity overlying cortical bone suggestive of a hematoma, and the latter defined as independent thickening of the periosteum, as measured from the outer most layer of periosteum to the inner most layer. Periosteal elevation was defined as sonographic separation of periosteum from cortical bone. A positive diagnosis of BSI by USI was designated as 2 out of the 8 aforementioned positive sonographic biomarkers based on the Bianchi paper as discussed above.

Table 1. Ultrasound Imaging Data Collection Sheet

Sonographic Finding	Yes/No	Severity (Denote or Circle)
1. Periosteal thickening		Thickness in mm
2. Calcified bone callus		NA
3. Cortical irregularities		1, minimal; 2, medium; 3, severe
4. Subcutaneous edema		1, minimal; 2, medium; 3, severe
5. Hypervascularity (color Doppler)		
Periosteum		1, minimal; 2, medium; 3, severe
Subcutaneous		1, minimal; 2, medium; 3, severe
Intraosseous		1, minimal; 2, medium; 3, severe
6. Hypervascularity (power Doppler)		
Periosteum		1, minimal; 2, medium; 3, severe
Subcutaneous		1, minimal; 2, medium; 3, severe
Intraosseous		1, minimal; 2, medium; 3, severe
7. Complete cortical disruption		NA
8. Periosteal elevation		NA
9. Periosteal hypoechogenicity		1, minimal; 2, medium; 3, severe

Statistical Analysis

Descriptive statistics of the demographic characteristics of the sample were examined using mean and standard deviation for age and sport, as well as bone type. The primary analysis examined the sensitivity, specificity, positive predictive value, and negative predictive value of USI diagnosis of BSI compared to MRI diagnosis of BSI at baseline. Secondary analyses examined MRI diagnosis of BSI compared to the USI measures at baseline. Exploratory univariate and multivariate logistic regression models examined the association between MRI diagnosis and each USI measure with multivariate models adjusting for BSI and location of bone injury. Significance was set at $P < .05$. All analyses were conducted in R[38] and Rstudio.[39] Sensitivity, specificity, and positive and negative predictive values were calculated using the epiR[40] package. Univariate and multivariate regression models were conducted using the glm command.

Results

Demographics

Characteristics of the participants are available in Appendix A including age, gender, and sport, as well

Table 2. Demographic Characteristics of Participants ($n = 37$)

Characteristic	Mean (SD)	Frequency (%)
Gender		
Female	31	84%
Male	6	16%
Age	20.62 (2.97)	
Sport		
Crew		3 (8%)
Equestrian		2 (5%)
Field hockey		2 (5%)
Gymnastics		4 (11%)
Lacrosse		1 (3%)
Running		15 (41%)
Soccer		2 (5%)
Tennis		2 (5%)
Track		1 (3%)
Volleyball		5 (14%)
Bone		
Fibula		4 (11%)
Medial cuneiform		1 (3%)
Metatarsal		20 (54%)
Tibia		13 (32%)

as clinical characteristics such as location of bone injury and history of prior BSI. There were 37 participants in the study: 31 women (84%) and 6 men with an age range of 18 to 33 years old (mean age = 20.62 years old, standard deviation [SD] = 2.97; Table 2). The most common sport was running (41%). There were 15 runners, 5 volleyball players, 4 gymnasts, 3 crew members, and 10 other athletes. Twelve participants (32%) had received traditional treatment for a previous BSI, 4 of whom had their repeat BSI in the same anatomical location as their previous BSI; however, all participants had completely recovered clinically from the prior BSI injury, and in this study demonstrated new MRI findings consistent with an acute BSI.

Ultrasonographic Assessment

The most common locations of suspected BSIs included the metatarsals ($n = 20$, 54%), tibia bone ($n = 13$, 32%), and fibula ($n = 4$, 11%). (Table 2). Regarding pain condition, 28 (76%) participants had pain on bony palpation on exam, 17 (46%) had pain with percussion on exam, and 8 (22%) reported pain in resting conditions. Pain with walking was reported by 23 participants (62%). MRI diagnosed BSIs in 30 out of the 37 participants (81%), while USI diagnosed BSIs in 26 participants (70%). There were two participants that were diagnosed as having a tibial BSI on USI, but were deemed to be negative on MRI. Both of these occurrences were in the tibia bone. USI diagnostic accuracy for BSIs confirmed by MRI was 78.4%.

Ultrasonographic Detections

According to our USI findings, periosteal thickening was detected in 27 BSIs (72.9%), calcified bone callus in 8 participants (21.6%), and cortical irregularities in 22 participants (59.5%). Periosteal thickening was detected in both USI and MRI studies. When fluid was present around the BSI site, it was depicted on MRI as a high intensity signal adjacent to the bone surface on T2 weighted images, and as a hypoechogenic area on USI (Figure 1A–C).

Subcutaneous edema was the most frequently reported positive BSI diagnostic finding on USI, noted in 30 (81.1%) of participants. Longitudinal B-mode imaging of BSI demonstrated subcutaneous edema and periosteal thickness as seen on the metatarsal in Figure 2. Axial B-mode imaging of the tibia demonstrated cortical irregularities and trace fluid on the surface of the bone, visualized in Figure 3. Hypervascularity measured by color or power Doppler in the periosteum or subcutaneous areas was detected in three participants under USI at site of BSI (Figure 4). Only one participant (2.7%) had evidence on USI of true cortical break corresponding to that of an MRI Grade 4b of BSI (Figure 5). Nineteen participants (51.4%) images depicted periosteal elevation (Figure 6), while 25 participants (67.6%) had periosteal hypoechogenicity (Figure 7).

Sensitivity and Specificity of USI Detection

Sensitivity and specificity of pain on bony palpation on exam in determining positive BSI diagnosis was 87% (95% CI, 0.69–0.96) and 71% (95% CI, 0.29–0.96) respectively (Table 3). Compared to MRI, overall USI was 80% (95% CI, 0.61–0.92) sensitive and 71% (95% CI, 0.29–0.96) specific in detecting BSI, with positive predictive value of 0.92 (95% CI, 0.75–0.99) and negative predictive value of 0.45 (95% CI, 0.17–0.77). Among USI diagnostic biomarkers, periosteal thickening had the highest combined sensitivity 80% (95% CI, 0.61–0.92) and specificity 57% (95% CI, 0.18–0.90). Pain on bony palpation (87%) and subcutaneous edema (83%)

Figure 1. Coronal MRI PD FS of the foot (**A**) demonstrating mild marrow edema with cortical thickening and periosteal edema along the medial aspect of the distal 2nd metatarsal diaphysis (white arrow). Axial MRI T1 (**B**) T2 FS (**C**) with evidence of stress reaction of the 2nd metatarsal middle to distal diaphysis with mild periosteal reaction. In the same patient, Axial B-mode imaging (**D**) depicting cortical irregularities (white arrow) and adjacent fluid (white arrowhead) in the absence of hypervascularity with power Doppler. Longitudinal B-mode imaging of the metatarsal BSI (**E**) showing irregular hypoechogenicity of periosteum (white arrowhead) as well as periosteal edema with periosteal thickness (white arrow).

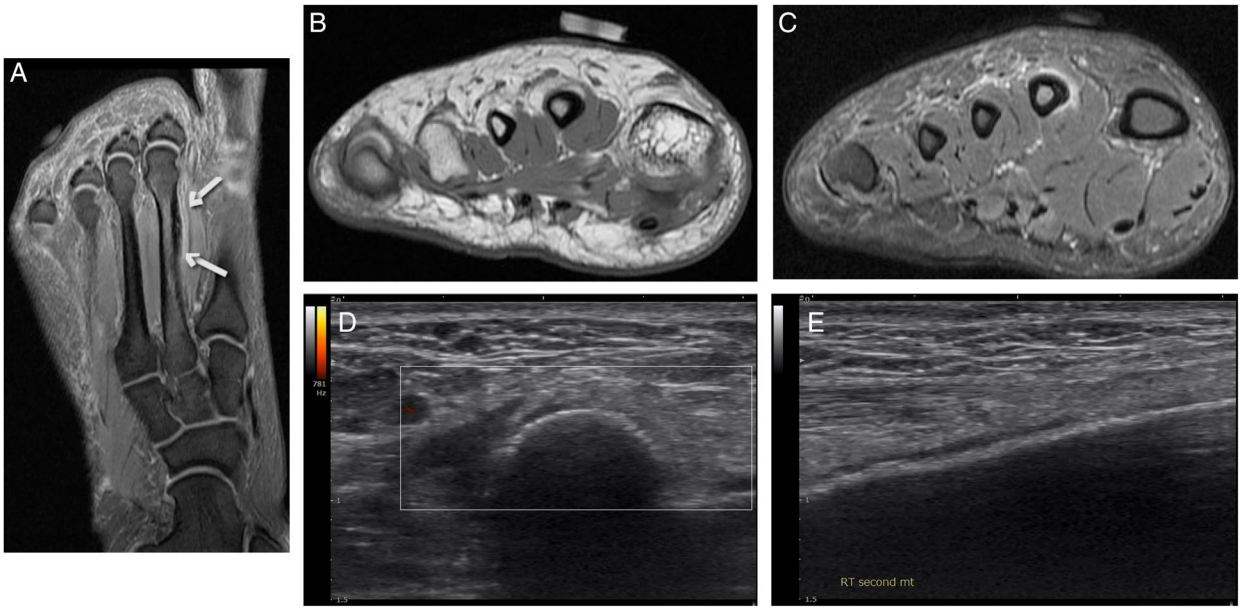

were the most sensitive, while calcified bone callus (100%), periosteal elevation (86%) and cortical irregularities (86%) were the most specific (Table 4).

Figure 2. Longitudinal B-mode imaging of the metatarsal BSI demonstrating periosteal edema and thickness (white arrow) with concurrent subcutaneous edema (white asterisk).

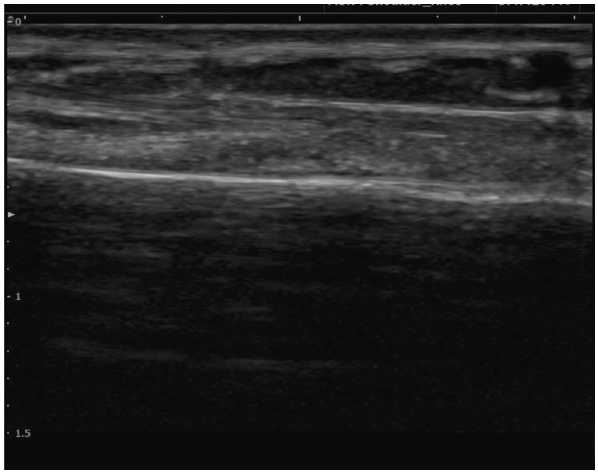

Univariate and Multivariate Regression Analyses

The univariate logistical regression models indicated that ultrasound diagnosis ($P = .016$), cortical irregularities ($P = .022$), and pain on bony palpation ($P = .005$) were significantly associated with MRI diagnosis (Table 4). Ultrasound diagnosis ($P = .020$), periosteal thickening ($P = .022$), cortical irregularities ($P = .029$) and pain on bony palpation ($P = .012$) were significant after adjusting for location of bone injury. There were no other significant measures that demonstrated a statistically significant association with MRI diagnosis.

Discussion

The current study suggests that USI is a potentially useful tool used in the diagnosis of BSI with a sensitivity of 80% and specificity of 71%. Our findings align closely with several previous studies that have been published on the topic. We found that periosteal thickening demonstrated the highest sensitivity and

Figure 3. A, Axial B-mode imaging of the healthy tibia without cortical irregularities. **B**, Axial B-mode imaging of the tibial BSI with cortical irregularities, in addition to trace edema overlying the bone. **C**, Longitudinal B-mode imaging of the tibial BSI with periosteal edema, thickness and cortical irregularities. **D**, Longitudinal power Doppler imaging of the tibial BSI depicting periosteal edema, thickness and cortical irregularities without hypervascularity.

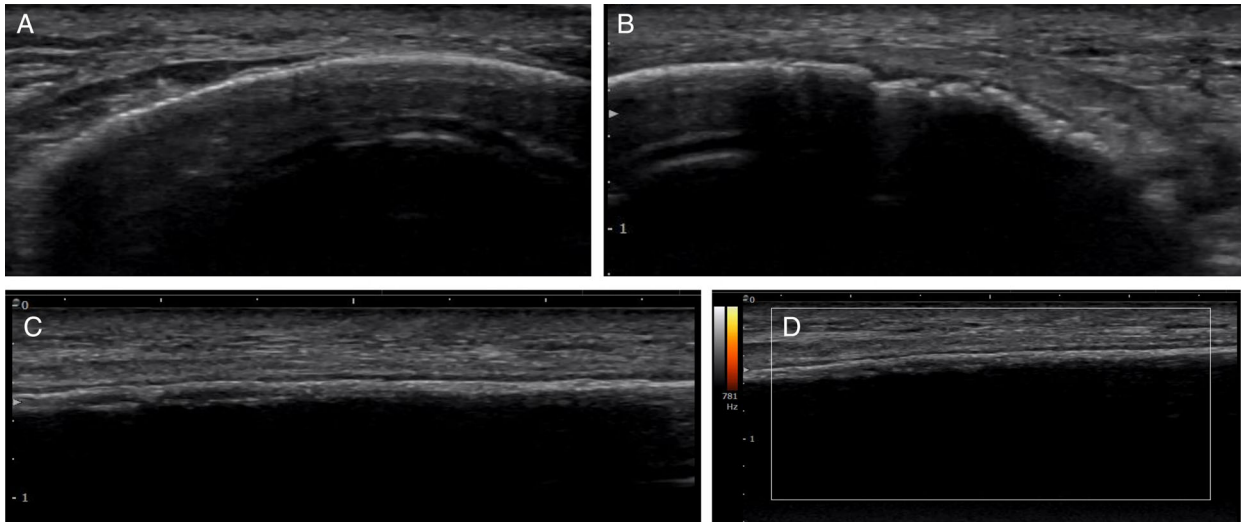

specificity for detecting BSI via USI, while periosteal elevation (Figure 6) and calcified bone callus (Figure 7) showed the highest specificity. This is important to note, because periosteal reaction presenting as thickening is typically a result of early bone stress and as described in the MRI classification system aligns with a Grade 1 Fredericson/Nattiv Score.[41] As described in a previous review article, the cortical reaction of BSIs is limited to the periosteum area which can be detected by USI.[10] We conclude that periosteal thickening is the most sensitive and specific biomarker in detection of BSIs by USI, and may also serve a pivotal role in longer-term follow-up care imaging.

Figure 4. Longitudinal B-mode imaging of metatarsal BSI with evidence of periosteum elevation (white arrowhead) and color Doppler imaging of the metatarsal BSI shows hypervascularity in the periosteum.

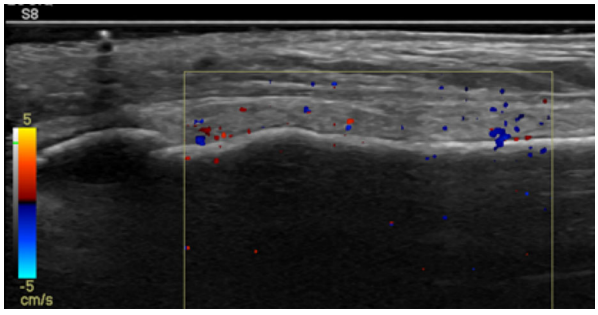

There were two false positive BSIs in this current study that had been diagnosed on USI but were negative with confirmatory MRI. Both of these cases occurred within the tibia. In contrast, Banal et al[29] in 2009 reported no false positives in their study of metatarsal bones, coinciding with an overall sensitivity of 83% and specificity of 76% for BSI diagnosis with USI. Such a discrepancy suggests that the accuracy of USI diagnosis in BSIs may be dependent in part to the anatomical location. The most frequent site of occurrence was that of the metatarsal bones, followed by the tibia, which is congruent with previous literature. Pester et al42 in 1992, for example, conducted a study evaluating lower extremity BSI incidence among 1338 military cases in which the most common locations were the metatarsals (66%), followed by the lower leg (13%) for males, with similar results in females. We acknowledge that we excluded BSIs in the hip and pelvis due to the limited ability of USI to diagnose deep bone structures and lack of periosteum at the hip and pelvis.[43] Alternatively, lower frequency curvilinear probes may be considered for the femur, but further research in this area to determine the accuracy is warranted.[44]

Figure 5. A, Axial B-mode imaging depicts complete cortical disruption (white arrow) and fluid (white arrowhead) in subcutaneous soft tissue. **B**, Axial power Doppler imaging demonstrates hypervascularity at the BSI site. **C** and **D**, Longitudinal B-mode imaging of the metatarsal BSI shows complete cortical disruption with hypoechogenicity of periosteum and (**E**) power Doppler demonstrates hypervascularity.

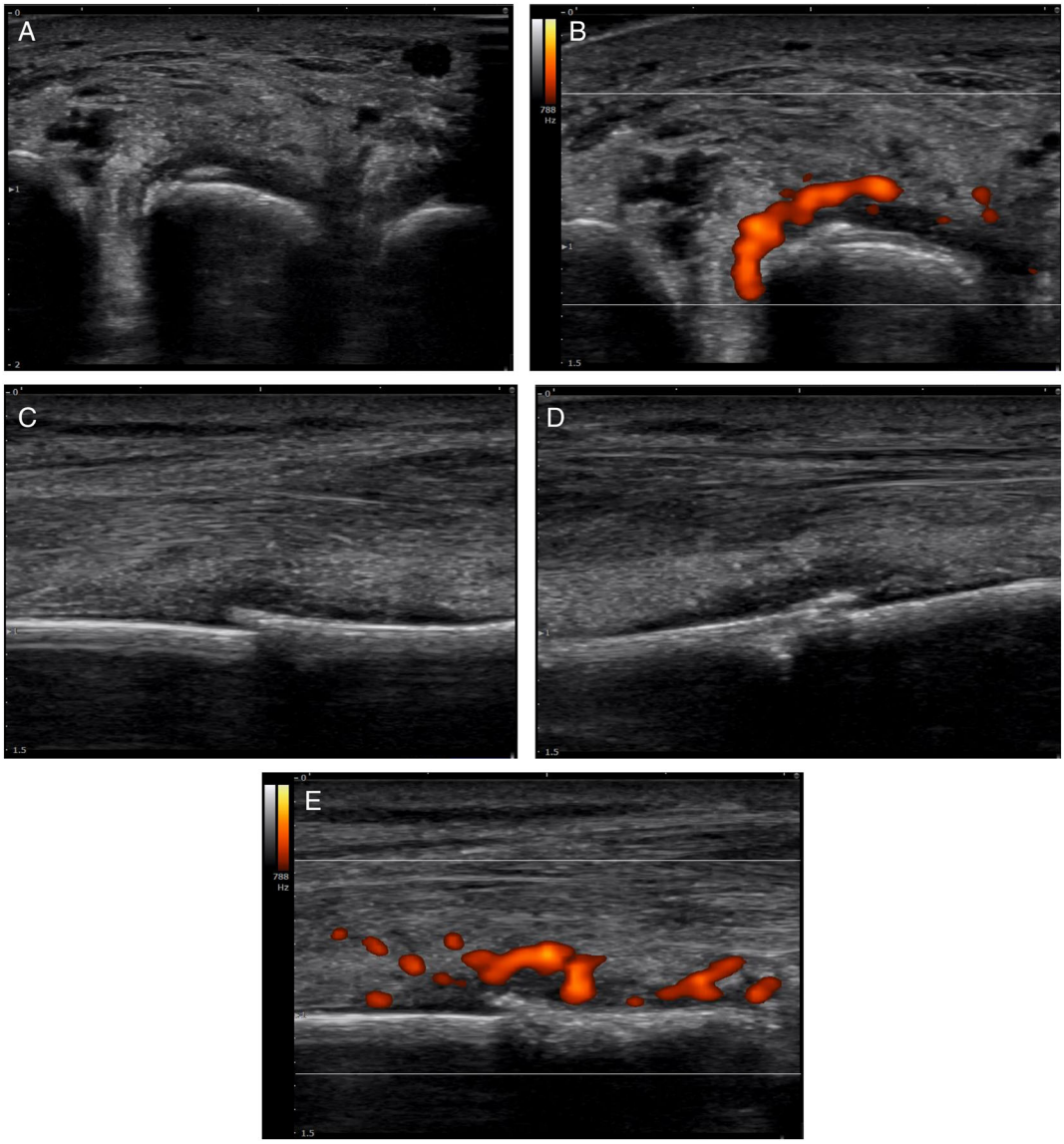

It is also noteworthy that our study only had three positive cases of hypervascularity (Figure 4), which has been portrayed in the literature as a signature of BSI diagnosis following fracture healing and callus formation.[45,46] Given the concurrent findings of periosteal thickening, cortical irregularity, periosteal elevation and hypoechogenicity in these patients, it can be postulated that hypervascularity may represent residual inflammation present within the soft tissue around the BSI as well as reactional periostitis. Of note, there were no hypervascularity changes detected intraosseous. This is likely because the frequency of diagnostic USI, commonly between 3 and 20 MHz does not have the energy to penetrate mature cortical bone, making it impossible to evaluate intraosseous bone with our current diagnostic ultrasound techniques.

Figure 6. A, Longitudinal B-mode imaging of a metatarsal BSI showing periosteal elevation (white arrowhead) and subcutaneous edema (asterisk). **B**, Magnified view of periosteal elevation and subcutaneous edema.

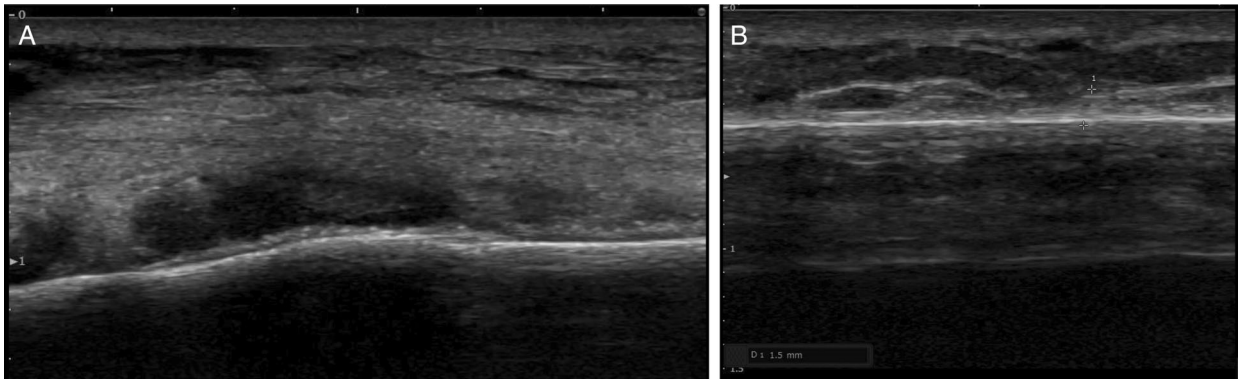

Figure 7. A and **B**, Longitudinal B-mode imaging of a metatarsal BSI showing calcified bone callus 2 weeks following onset of symptoms. **C**, Color Doppler without any evidence of hypervascularity.

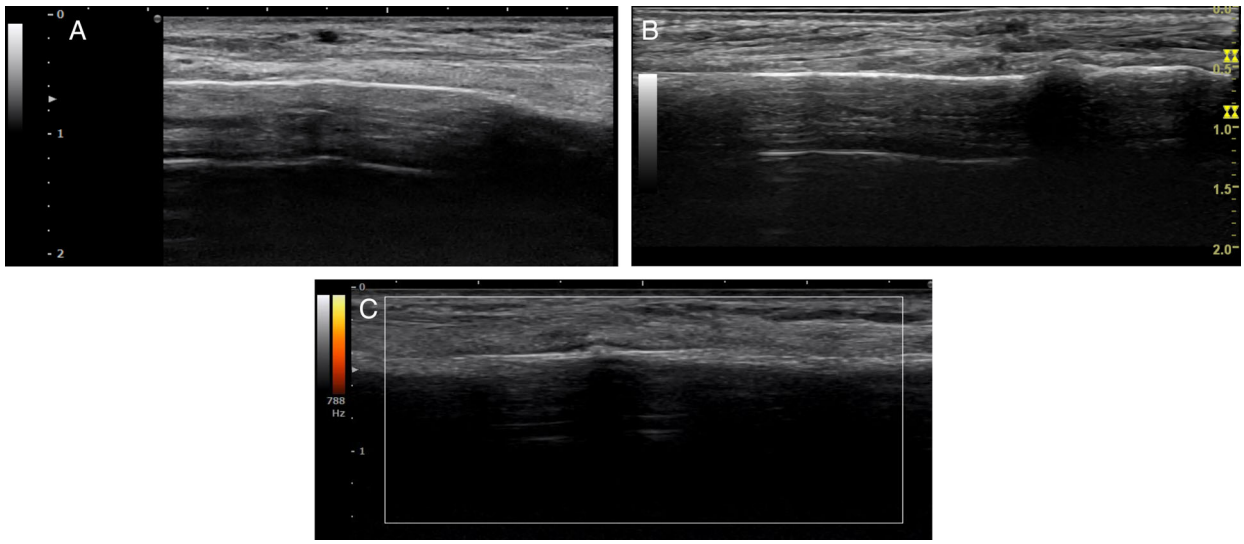

Interestingly, pain on bony palpation had slightly better sensitivity and equivalent specificity as USI diagnosis of BSI, when compared to the reference standard of MRI. These data highlight the importance of a simple and no-cost physical examination test in the diagnosis of BSI. However, as this test is binary, it does have limitations in further study as it relates to grading, prognosis and return to sport following a BSI. On the contrary, ultrasound has many sonographic biomarkers, some of which are quantitative such as the measurement of periosteal thickness, that may help elucidate the progression of BSI over time. Furthermore, using both pain on bony palpation and sonographic findings together in the diagnostic algorithm may produce a more accurate diagnosis. Using both metrics may be specifically helpful in those patients with a history of previous BSI at the same anatomic site of new concern. Within the study, there were four subjects that had a previous BSI at the same site of new BSI. Further research is needed to establish both MRI and sonographic evolution of a healing and healed BSI, denoting if any biomarkers persist after full resolution.

Table 3. Sensitivity and Specificity of Ultrasound Test and Other Measures Compared to the MRI at Baseline

	MRI—Positive BSI	MRI—Negative BSI	Sensitivity (95% CI)	Specificity (95% CI)	PPV (95% CI)	NPV (95% CI)
Ultrasound			80	71	92	45
Positive BSI	24	2	(61–92)	(29–96)	(75–99)	(17–77)
Negative BSI	6	5				
Periosteal thickening			80	57	89	40
Positive BSI	24	3	(61–92)	(18–90)	(71–98)	(12–74)
Negative BSI	6	4				
Cortical irregularities			70	86	95	40
Positive BSI	21	1	(51–85)	(42–100)	(77–100)	(16–68)
Negative BSI	9	6				
Subcutaneous edema			83	29	83	29
Positive BSI	25	5	(65–94)	(4–71)	(65–94)	(4–71)
Negative BSI	5	2				
Periosteal elevation			60	86	95	33
Positive BSI	18	1	(41–77)	(42–100)	(74–100)	(13–59)
Negative BSI	12	6				
Periosteal hypoechogenicity			70	43	84	25
Positive BSI	21	4	(51–85)	(10–82)	(64–95)	(5–57)
Negative BSI	9	3				
Pain on bony palpation			87	71	93	56
Positive BSI	26	2	(69–96)	(29–96)	(76–99)	(21–86)
Negative BSI	4	5				
Calcified bone callus			27	100	100	24
Positive BSI	8	0	(12–44)	(59–100)	(63–100)	(10–42)
Negative BSI	22	7				

Abbreviations: BSI, bone stress injury; CI, confidence interval; PPV, positive predicted value; NPV, negative predicted value.

Table 4. Exploratory Univariate and Multivariate Logistic Regression Models Examining the Association Between Positive Magnetic Resonance Imaging Diagnosis and Other Bone Measures at Baseline

	Univariate Models		Multivariate Models[a]	
	Estimate (SE)	*P* Value*	Estimate (SE)	*P* Value*
Ultrasound diagnosis	2.30 (0.95)	0.016	2.28 (0.98)	0.020
Periosteal thickening	1.67 (0.89)	0.060	2.25 (0.98)	0.022
Cortical irregularities	2.64 (1.15)	0.022	2.55 (1.17)	0.029
Subcutaneous edema	0.69 (0.97)	0.475	0.64 (1.02)	0.531
Periosteal elevation	2.20 (1.14)	0.055	2.03 (1.16)	0.080
Periosteal hypoechogenicity	0.56 (0.86)	0.516	0.79 (0.91)	0.390
Pain on bony palpation	2.79 (0.99)	0.005	2.58 (1.03)	0.012

[a]Multivariate models adjust for bone injuries and days to onset. SE, standard error.
*$P < .05$.

There are many advantages to USI over MRI, including its dynamic practicality, which provides the treating clinician with an opportunity to evaluate local soft tissue sites in real-time. USI takes significantly less time than an MRI to perform, between 10 and 20 min in this present study, and can be done as part of the clinical examination. Risk factors for lower extremity BSIs include repetitive motions that exacerbate muscle fatigue or aggravate previous injuries, thus having the ability to assess tendons and ligaments which attach to the periosteum can be extremely beneficial.[47] In addition, localizing the origin of pain using sonopalpation during diagnostic scanning can also be quite helpful in discerning the

etiology from that of an alternative pathology, such as chronic exertional compartment syndrome.[48,49] Lastly, more often in the pediatric population, completing an MRI may often times require sedation; thus, using bedside ultrasound in the interim or alternatively can prove to be quite useful, especially when evaluating for fracture and BSI. Several prior studies have touted USI's accurate capability of demonstrating cortical break and evaluating for displacement. Eckert et al[50] in 2015 showed that distal forearm fractures can be diagnosed by ultrasound with a sensitivity of 96% and specificity of 97%, while supracondylar fractures are also highly sensitive to USI as well.[51] In our study, one case demonstrated true cortical break on USI (Figure 5) that corresponded to a Grade 4 injury on the Fredericson & Nattiv MRI classification system.

Potential limitations of our study include limited generalizability. The subjects represent only a sector of the general patient population. As an effect of the practice setting, many of the subjects were young and healthy college-level athletes, contributing to the study's high prevalence of 81% (30/37). The high prevalence likely impacted the high PPV and low NPV. With this in mind, our study results of a high PPV indicates a high likelihood of a true diagnosis of BSI; alternatively, a negative test should be followed by MRI given the low NPV. In follow-up research, it would be interesting to test ultrasound in the diagnosis of BSI in a less prevalent population.

Secondary to the limited number of subjects, the confidence intervals in the regression analysis are large, indicating uncertainty. Further study is needed with larger recruitment. Another limitation in this study was the fact that we had multiple sonologists performing the scans without examination of inter-rater reliability; however, for each scan, the study included two examiners blinded to each other's measurements, and when interpretation diverged, a third examiner acted as a tie-breaker. Additionally, all sonologists were well-trained in ultrasound.

In summary, USI may be a point-of-care tool for the current practicing sports medicine provider to combine with their clinical evaluation in the diagnosis of BSIs of the lower extremity. Of the cortical surface biomarkers evaluated, periosteal thickening has proven to be most reliable and should be incorporated into all USI BSI diagnostic criteria sets. Findings of periosteal elevation and calcified bone callus carry a high PPV, and when present should indicate a high likelihood of a true diagnosis of BSI. Additional research is ongoing to determine the role of USI in follow-up care and return-to-play protocol.

References

1. Fredericson M, Jennings F, Beaulieu C, Matheson GO. Stress fractures in athletes. *Top Magn Reson Imaging TMRI* 2006; 17:309–325. https://doi.org/10.1097/RMR.0b013e3180421c8c.
2. Rauh MJ, Macera CA, Trone DW, Shaffer RA, Brodine SK. Epidemiology of stress fracture and lower-extremity overuse injury in female recruits. *Med Sci Sports Exerc* 2006; 38:1571–1577. https://doi.org/10.1249/01.mss.0000227543.51293.9d.
3. Barrack MT, Gibbs JC, De Souza MJ, et al. Higher incidence of bone stress injuries with increasing female athlete triad-related risk factors: a prospective multisite study of exercising girls and women. *Am J Sports Med* 2014; 42:949–958. https://doi.org/10.1177/0363546513520295.
4. Field AE, Gordon CM, Pierce LM, Ramappa A, Kocher MS. Prospective study of physical activity and risk of developing a stress fracture among preadolescent and adolescent girls. *Arch Pediatr Adolesc Med* 2011; 165:723–728. https://doi.org/10.1001/archpediatrics.2011.34.
5. Robertson GA, Wood AM. Lower limb stress fractures in sport: optimizing their management and outcome. *World J Orthop* 2017; 8:242–255
6. Iwamoto J, Sato Y, Takeda T, Matsumoto J. Analysis of stress fractures in athletes based on our clinical experience. *World J Orthop* 2011; 2:7–12. https://doi.org/10.5312/wjo.v2.i1.7.
7. Pegrum J, Dixit V, Padhiar N, Nugent I. The pathophysiology, diagnosis, and management of foot stress fractures. *Phys Sportsmed* 2014; 42:87–99. https://doi.org/10.3810/psm.2014.11.2095.
8. McBryde AM. Stress fractures in athletes. *J Sports Med* 1975; 3: 212–217.
9. Matheson GO, Clement DB, McKenzie DC, Taunton JE, Lloyd-Smith DR, MacIntyre JG. Stress fractures in athletes. A study of 320 cases. *Am J Sports Med* 1987; 15:46–58. https://doi.org/10.1177/036354658701500107.
10. Fukushima Y, Ray J, Kraus E, Syrop IP, Fredericson M. A review and proposed rationale for the use of ultrasonography as a diagnostic modality in the identification of bone stress injuries. *J Ultrasound Med Off J Am Inst Ultrasound Med* 2018; 37:2297–2307. https://doi.org/10.1002/jum.14588.
11. Song SH, Koo JK. Bone stress injuries in runners: a review for raising interest in stress fractures in Korea. *J Korean Med Sci* 2020; 34:e38.

12. Tenforde AS, Kraus E, Fredericson M. Bone stress injuries in runners. *Phys Med Rehabil Clin N Am* 2016; 27:139–149.
13. Kijowski R, Choi J, Mukharjee R, de Smet A. Significance of radiographic abnormalities in patients with tibial stress injuries: correlation with magnetic resonance imaging. *Skeletal Radiol* 2007; 36: 633–640.
14. Matcuk GR, Mahanty SR, Skalski MR, Patel DB, White EA, Gottsegen CJ. Stress fractures: pathophysiology, clinical presentation, imaging features, and treatment options. *Emerg Radiol* 2016; 23:365–375.
15. Sofka CM. Imaging of stress fractures. *Clin Sports Med* 2006; 25: viii.
16. Martin SD, Healey JH, Horowitz S. Stress fracture MRI. *Orthopedics* 1993; 16:75–78.
17. Hodler J, Steinert H, Zanetti M, et al. Radiographically negative stress related bone injury. MR imaging versus two-phase bone scintigraphy. *Acta Radiol Stockh Swed* 1998; 39:416–420.
18. Dobrindt O, Hoffmeyer B, Ruf J, et al. MRI versus bone scintigraphy evaluation for diagnosis and grading of stress injuries. *Nuklearmedizin* 2012; 51:88–94.
19. Arendt EA, Griffiths HJ. The use of MR imaging in the assessment and clinical management of stress reactions of bone in high-performance athletes. *Clin Sports Med* 1997; 16:291–306.
20. Fredericson M, Bergman AG, Hoffman KL, Dillingham MS. Tibial stress reaction in runners. Correlation of clinical symptoms and scintigraphy with a new magnetic resonance imaging grading system. *Am J Sports Med.* 1995; 23:472–481. https://doi.org/10.1177/036354659502300418.
21. Adrent EA, Griffiths HJ. The use of MR imaging in the assessment and clinical management of stress reactions of bone in high-performance athletes. *Clin Sports Med* 1997; 16:291–306.
22. Nattiv A, Kennedy G, Barrack MT, et al. Correlation of MRI grading of bone stress injuries with clinical risk factors and return to play: a 5 year prospective study in collegiate track and field athletes. *Am J Sports Med* 2013; 41:1930–1941.
23. Kijowski R, Choi J, Shinki K, Del Rio AM, Smet D. Validation of MRI classification system for tibial stress injuries. *AJR Am J Roentgenol* 2012; 198:878–884. https://doi.org/10.2214/AJR.11.6826.
24. Howard CB, Lieberman N, Mozes G, Nyska M. Stress fracture detected sonographically. *AJR Am J Roentgenol* 1992; 159:1350–1351. https://doi.org/10.2214/ajr.159.6.1442422.
25. Griffith JF, Rainer TH, 0Ching AS, Law KL, Cocks RA, Metreweli C. Sonography compared with radiography in revealing acute rib fracture. *AJR Am J Roentgenol* 1999; 173:1603–1609
26. Caruso G, Lagalla R, Derchi L, Iovane A, Sanfilippo A. Monitoring of fracture calluses with color Doppler sonography. *J Clin Ultrasound* 2000; 28:20–27.
27. Rawool NM, Goldberg BB, Forseberg F, Winder AA, Hume E. Power Doppler assessment of vascular changes during fracture treatment with low-intensity ultrasound. *J Ultrasound Med* 2003; 22:145–153.
28. Bodner G, Stöckl B, Fierlinger A, Schocke M, Bernathova M. Sonographic findings in stress fractures of the lower limb: preliminary findings. *Eur Radiol* 2005; 15:356–359. https://doi.org/10.1007/s00330-004-2525-8.
29. Banal F, Gandjbakhch F, Foltz V, et al. Sensitivity and specificity of ultrasonography in early diagnosis of metatarsal bone stress fractures: a pilot study of 37 patients. *J Rheumatol* 2009 Aug; 36: 1715–1719.
30. Bianchi S, Luong DH. Stress fractures of the calcaneus diagnosed by sonography. *J Ultrasound Med* 2018; 37:521–529.
31. Farkash U. Ultrasonography as diagnostic modality of tibiae stress fractures. *J Musculoskelet Res* 2008; 11:55–61.
32. Wright AA, Hegedus EJ, Lenchik L, Kuhn KJ, Santiago L, Smoliga JM. Diagnostic accuracy of various imaging modalities for suspected lower extremity stress fractures: a systamtic review with evidence-based recommendations for clinical practice. *Am J Sports Med* 2016; 44:255–263.
33. Arni D, Lambert V, Delmi M, Bianchi S. Insufficiency fracture of the calcaneum: sonographic findings. *J Clin Ultrasound* 2009; 37: 424–427.
34. Banal F, Etchepare F, Rouhier B, et al. Ultrasound ability in early diagnosis of stress fracture of metatarsal bone. *Ann Rheum Dis* 2006; 65:977–978.
35. Su DCJ, Chang KV. Mid-foot cellulitis? Ultrasound imaging of stress fracture at the third metatarsal bone. *Kaohsiung J Med Sci* 2016; 32:162–163.
36. Hoglund LT, Silbernagel KG, Taweel NR. Distal fibular stress fracture in a female recreational runner: a case report with musculoskeletal ultrasound imaging findings. *Int J Sports Phys Ther* 2015; 10:1050–1058.
37. Kyh V, Wyssa B, Bianchi S. Bilateral stress fracture of the tibia diagnosed by ultrasound: a case report. *J Ultrasound* 2012; 15: 130–134.
38. Mark Stevenson with contributions from Telmo Nunes, Cord Heuer, Jonathon Marshall, Javier Sanchez, Ron Thornton, Jeno Reiczigel, Jim Robison-Cox, Paola Sebastiani, Peter Solymos, Kazuki Yoshida, Geoff Jones, Sarah Pirikahu, Simon Firestone, Ryan Kyle, Johann Popp, Mathew Jay and Charles Reynard. (2020). epiR: Tools for the Analysis of Epidemiological Data. R package version 1.0-14. https://CRAN.R-project.org/package=epiR.
39. R Core Team. *R: A Language and Environment for Statistical Computing*. Vienna, Austria: R Foundation for Statistical Computing; 2020 https://www.R-project.org/.
40. RStudio Team. *RStudio: Integrated Development for R*. Boston, MA: RStudio, Inc.; 2019 http://www.rstudio.com/.
41. Fredericson M, Bergman AG, Hoffman KL, Dillingham MS. Tibial stress reaction in runners. Correlation of clinical symptoms and

scintigraphy with a new magnetic resonance imaging grading system. *Am J Sports Med* 1995; 23:472–481. https://doi.org/10.1177/036354659502300418.

42. Pester S, Smith PC. Stress fractures in the lower extremities of soldiers in basic training. *Orthop Rev* 1992; 21:297–303.
43. Perez González M, Velázquez Fragua P, López Miralles E, Abad Moretón MM. Rare stress fracture: longitudinal fracture of the femur. *Radiologia* 2018; 60:262–266. https://doi.org/10.1016/j.rx.2017.07.004.
44. Steele CE, Cochran G, Renninger C, Deafenbaugh B, Kuhn KM. Femoral neck stress fractures: MRI risk factors for progression. *J Bone Joint Surg Am* 2018; 100:1496–1502. https://doi.org/10.2106/JBJS.17.01593.
45. Caruso G, Lagalla R, Derchi L, Iovane A, Sanfilippo A. Monitoring of fracture calluses with color Doppler sonography. *J Clin Ultrasound* 2000; 28:20–27.
46. Arni D, Lambert V, Delmi M, Bianchi S. Insufficiency fracture of the calcaneum: sonographic findings. *J Clin Ultrasound* 2009; 37:424–427. https://doi.org/10.1002/jcu.2057.
47. Ramponi DR, Hedderick V, Maloney SC. Metatarsal stress fractures. *Adv Emerg Nurs J* 2017; 39:168–175. https://doi.org/10.1097/TME.0000000000000154.
48. Winters M, Bakker EWP, Moen MH, Barten CC, Teeuwen R, Weir A. Medial tibial stress syndrome can be diagnosed reliably using history and physical examination. *Br J Sports Med* 2018; 52:1267–1272. https://doi.org/10.1136/bjsports-2016-097037.
49. Bresler M, Mar W, Toman J. Diagnostic imaging in the evaluation of leg pain in athletes. *Clin Sports Med* 2012; 31:217–245. https://doi.org/10.1016/j.csm.2011.09.006.
50. Eckert K, Ackermann O. Sonographic fracture diagnostics. *Radiologe* 2015; 55:355–368. https://doi.org/10.1007/s00117-015-0003-8.
51. Eckert K, Janssen N, Ackermann O, Schweiger B, Radeloff E, Liedgens P. Ultrasound diagnosis of supracondylar fractures in children. *Eur J Trauma Emerg Surg Off Publ Eur Trauma Soc* 2014; 40:159–168. https://doi.org/10.1007/s00068-013-0306-2.

Appendix A

Demographic Characteristics of Participants

BSI	Age	Sex	Sports	Bone
1	23	Female	Equestrian	Metatarsal
2	23	Female	Equestrian	Metatarsal
3	20	Female	Soccer	Tibia
4	18	Male	Gymnastics	Tibia
5	18	Male	Gymnastics	Tibia
6	19	Female	Crew	Tibia
7	33	Female	Running	Tibia
8	22	Female	Running	Metatarsal
9	20	Female	Running	Metatarsal
10	20	Female	Running	Metatarsal
11	20	Female	Running	Tibia
12	25	Female	Running	Metatarsal
13	25	Female	Running	Metatarsal
14	21	Female	Running	Tibia
15	18	Male	Running	Metatarsal
16	18	Male	Running	Metatarsal
17	20	Female	Volleyball	Tibia
18	20	Female	Volleyball	Metatarsal
19	20	Female	Volleyball	Metatarsal
20	18	Female	Running	Metatarsal
21	20	Female	Running	Metatarsal
22	18	Female	Gymnastics	Fibula
23	27	Female	Running	Metatarsal
24	18	Female	Running	Metatarsal
25	20	Female	Running	Metatarsal
26	21	Female	Rowing	Tibia
27	19	Male	Gymnastics	Fibula
28	21	Female	Soccer	Metatarsal
29	21	Female	Field hockey	Metatarsal
30	19	Female	Volleyball	Fibula
31	20	Male	Tennis	Fibula
32	18	Female	Lacrosse	Metatarsal
33	20	Female	Field hockey	Tibia
34	19	Female	Volleyball	Metatarsal
35	20	Female	Crew	Tibia
36	21	Female	Tennis	Medial cuneiform
37	20	Female	Track	Tibia